https://dx.doi.org/10.1016/j.enbuild.2022.112765

A multi-agent system based coordinated multi-objective optimal load scheduling strategy using marginal emission factors for building cluster demand response

Hanbei Zhang[a], Fu Xiao[a,b,*], Chong Zhang[a], Rongling Li[c]

[a] *Department of Building Environment and Energy Engineering, The Hong Kong Polytechnic University, Kowloon, Hong Kong*

[b] *Research Institute for Smart Energy, The Hong Kong Polytechnic University, Kowloon, Hong Kong*

[c] *Department of Civil and Mechanical Engineering, Technical University of Denmark, Brovej, Building 118, 2800 Kgs Lyngby, Denmark*

Abstract: Building cluster load management to harness energy flexibility and reduce both electricity cost and carbon emissions is an important but inadequately addressed issue in the context of carbon neutrality. This study develops a multi-agent system (MAS) based coordinated optimal load scheduling strategy for building cluster load management in response to dynamic electricity price and marginal emission factor (MEF) simultaneously. The strategy effectively solves the multi-objective optimization problem of conflicts, i.e., minimizing the electricity cost, carbon emissions and peak load while maintaining a good level of users' satisfaction with electricity use quantified by a utility function. Case study on a campus building cluster is carried out to test the strategy developed. Three demand response (DR) schemes are designed for the building cluster, i.e., price-based DR, MEF-based DR, and the price and MEF hybrid-based DR which implements the optimal scheduling strategy developed. In addition, two real scenarios with opposite correlations between dynamic electricity price and MEF, i.e., positively correlated (scenario 1) and negatively correlated (scenario 2), are extracted from German electricity market. The electricity costs, carbon emissions, peak loads, and utility of the three DR schemes in the two scenarios are critically compared. The

* Corresponding author.
E-mail address: linda.xiao@polyu.edu.hk (F. Xiao).

results show that the price-based DR may result in the rise of carbon emissions, and the MEF-based DR may lead to higher electricity cost, depending on the correlation between dynamic electricity price and MEF. The optimal strategy developed can achieve a compromise between the conflicting objectives in both scenarios. Under the extremely disadvantageous situation like scenario 2, where the trends of the price and MEF are completely opposite, the price-based DR results in an increase of carbon emission of 2.78%, and the MEF-based DR leads to an increase of electricity cost of 2.63%. The hybrid-based DR can reduce the peak power by 5.54% without increasing electricity cost and carbon emissions in scenario 2. This research provides an effective optimal load scheduling strategy as well as the application guideline for building cluster DR management towards decarbonization and economic benefit.

Keywords: building cluster, marginal emission factors, multi-objective optimization, multi-agent system, demand response

Nomenclature

x_i^k	The load schedules of the individual building i in time slot k
L^k	The aggregated load schedules of the entire building cluster in time slot k
Pr_{wh}^k	The electricity prices in time slot k
MEF^k	The marginal emission factors in time slot k
$\bar{x}^k$	The energy imbalance in time slot k
λ^k	The Lagrange's multiplier in time slot k
C^k	The electricity cost in the time slot k
CE^k	The electricity-related carbon emission in time slot k
PL	The peak load of the building cluster
U_i^k	The utility function of building i for consuming electricity in time slot k
S_i^k	The sacrifice of utility
$x_{0,i}^k$	The load baseline of building i at time slot k
ω_i	The preference for electricity use of building i to shift the power load
$B_{up,i}^k$	The upper limit of flexible load capacity of building i at time slot k
α	The weighting factor of the electricity cost objective function
β	The weighting factor of the carbon emission objective function
γ	The weighting factor of the peak load objective function
θ	The weighting factor of the utility function objective function
ρ	The penalty factor of Augmented Lagrange's multiplier
s	The number of the iteration step
$\varepsilon_1, \varepsilon_2$	The pre-set stopping threshold
K	The total number of time slots in a day
N	The total number of individual buildings

1. Introduction

Demand response (DR), a key demand-side management strategy adopted by smart grids, is considered as a promising solution to harness energy flexibility[1,2], reduce peak power demand [3], and relieve power supply-demand imbalance in power grids[4,5]. Various DR programs such as incentive-based DR and price-based DR programs are launched to facilitate power consumers to adjust their power uses. The price-based DR programs usually adopt the dynamic pricing mechanism, which sets a high price during peak periods and a low price during off-peak periods, to flat the demand curve [6]. In such programs, power consumers are stimulated to change their normal demand profiles to benefit from the electricity price variations, i.e., to take advantage of lower-price periods and avoid higher-price periods [7].

As major power consumers, buildings consume over 90% of total electricity in Hong Kong [8] and about 40% of total energy use worldwide [9]. Buildings also have a considerable amount of flexible loads and capacities which are ideal for participating DR. For example, the electricity load for space cooling/heating could be shifted by taking advantage of building thermal mass [10] and active thermal storage [11]. Buildings can play a significant role in DR programs by adjusting their electrical power demands in response to the dynamic electricity prices[12,13]. According to the review conducted by Péan et al. [14], the great majority of published research on building DR consider economic optimization for price-based DR, in other words, the building power demand management strategies are commonly implemented to achieve electricity cost saving.

With the growing concern about carbon neutrality in recent years, an increasing number of researchers consider carbon emissions in the optimization strategies for building DR. The annual average carbon emission factors (CEFs) of grid electricity has been commonly adopted to evaluate the environmental effects of DR for building [15–17] and district energy system [18]. However, using annual average CEFs to evaluate the environmental effects of DR will lead to inaccurate estimation of carbon emissions due to the wide variations in emission factors of different types of fuels at different time periods [19]. The temporal granularity of CEFs should be considered for accurately

quantifying the realistic electricity-consumption-related carbon emission [20]. In view of this, some studies have adopted time-varying CEFs for estimating the carbon emissions, e.g., electricity mix emission factors (XEFs) [21,22]. XEF is the average emission factor of the mix of power generators at a given time and varies in different time intervals, as shown in Fig. 1. Lowry [21] used the hourly XEFs of the electricity grid in UK to implement building DR on the HVAC system for reducing overall carbon emissions. The whole year hourly XEFs from the Danish transmission system operator were used by Vogler-Finck et al. [22] in a model predictive controller to minimize the carbon emissions of heating system in a single-family house.

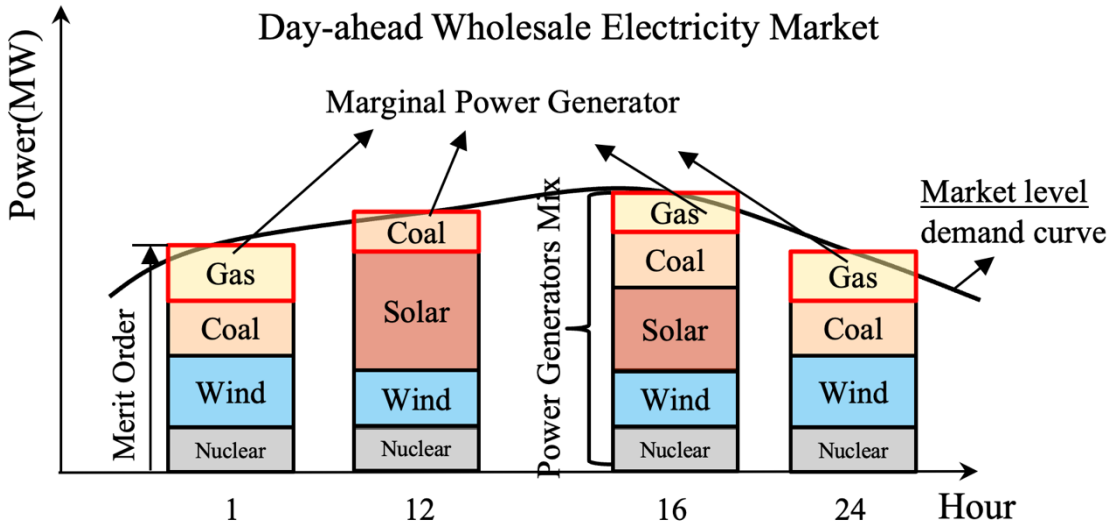

Fig. 1. Illustration of power generators mix and marginal power generator [20]

However, using XEFs for evaluating the effect of DR on carbon emissions may still lead to misleading results [23]. This is because XEFs assume all power generators react evenly to the load variations [24]. In fact, different generators have different reaction to the load variations. Fig. 1 illustrates the marginal power generators and the operation order of power generators (so-called merit order) to meet the market-level load demand in a day-ahead wholesale electricity market. The merit order is a way of ranking power generators in power system based on marginal cost and adjustability. The power generators with poor adjustability (e.g., nuclear power generators and coal-fired generators) or low marginal cost (e.g., photovoltaic and wind turbines) are the first ones to meet demand, and the generators with higher marginal cost (e.g. gas power generators) will be operated only when the output of the plants with poor adjustability

or low marginal cost cannot meet the loads. The marginal power generator at a given time is the one that has the lowest marginal cost and still has adjustable capacity [24] that can be used to respond to DR events. Thus, only the emission factors of marginal power generator will have influence on the emission calculation in the DR event, which means that using XEFs to evaluate the effect of DR on carbon emission is not accurate. Instead, the carbon emission factors of the marginal power plant, which is called marginal emission factors (MEFs) [20] should be used to estimate the carbon emission when load varies.

The energy flexibility of buildings needs to be harnessed through a cluster of buildings to produce a sufficient aggregated amount to make significant effects on electricity grid [1]. A building cluster is a group of buildings that can be managed in a coordinated way by an aggregator such as facility management company [25]. When each building independently carries out load scheduling strategy without effective coordination, it may cause critical safety issue for power grid, such as a sharp increase of aggregated load (called as aggregated peak load) during the period of low electricity price. Therefore, effective coordinated demand management of the building cluster is needed to prevent such safety issue and achieve aggregated benefits for power grid [26]. The multi-agent system (MAS) is one of the domains that deal with modeling multiple autonomous decision-making agents [27]. According to the definition in [28], each "agent" in MAS is an intelligent entity, which is placed in an environment and sense different parameters that are used to make a decision based on its own goal. The agent has the ability of being sociable, reactive and pro-active [29]. The efficiency of MAS to solve complex task stems from the division of computational labor inherent in MAS whereby a complex task is divided into multiple smaller tasks, each of which is assigned to a distinct agent [30]. Due to its powerful ability to capture the complex interactions between multiple agents [28] and solve complex tasks, MAS has been widely used in the field of computer science [31] and has gain attention in the field of micro-grid[32–35] and building energy system [36–38] for coordinated control and energy management. Hence, MAS is used in this study to achieve the building cluster demand management in a decentralized manner. Previous studies on MAS-based coordinated demand management mainly focused on minimizing the electricity cost [29,32] for price-based DR. In the context of carbon neutrality, how to achieve decarbonization

and guarantee economic benefit for building cluster load management should be clearly addressed. However, few study considers the MEFs and dynamic electricity prices simultaneously in the building cluster DR to achieve the decarbonization and economic goals at the same time. Moreover, as pointed out in [20], the hourly MEFs can be positively or negatively correlated with hourly dynamic electricity prices due to the varying output of renewable energy and merit order of power generators. The correlation between MEFs and dynamic electricity prices is a key factor when conducting DR to achieve both decarbonization and economic benefit. However, up to now, few studies have analyzed the impact of different correlations between MEFs and dynamic electricity prices on the performance of building cluster DR in terms of electricity cost, carbon emission, peak load, and users' satisfaction with electricity use.

Table 1 Comparison of this study with recent research work on similar topics

Refs.	Objectives				DR scheme			Scale	
	Electricity cost	Carbon emission	Peak load	Utility function	Price-based	MEF-based	Hybrid-based	Single building	Building cluster
[3]	√	×	√	√	×	×	×	×	√
[5]	√	×	×	√	×	×	×	×	√
[20]	√	√	×	×	√	√	×	√	×
[33]	√	×	×	×	√	×	×	×	√
[40]	√	√	√	×	√	√	×	√	×
[41]	√	×	×	√	√	×	×	√	×
[42]	√	×	×	√	√	×	×	×	√
[43]	√	×	√	√	×	×	×	√	×
[44]	√	×	√	√	√	×	×	×	√
[45]	√	×	×	×	√	×	×	√	×
[46]	√	×	×	√	√	×	×	√	×
[47]	√	×	√	√	√	×	×	√	×
[48]	√	×	√	×	×	×	×	×	√
[49]	√	×	√	×	√	×	×	√	×
This paper	√	√	√	√	√	√	√		√

Table 1 provides a comparison between the method proposed in this paper and recent studies. The research gaps are summarized as followed. First, previous studies of DR have solved the optimal load scheduling problem in the price-based DR scheme, but none has considered the marginal emission factors and dynamic electricity prices simultaneously, to the best of the authors' knowledge. There are a few studies considered carbon emissions and dynamic electricity price simultaneously; however,

the carbon emissions were usually measured by a fix emission factor which is unrealistic. Second, understanding of the influences of MEF and dynamic electricity price correlation on the performance of building cluster optimal load scheduling is limited. Third, there is little experience in formulating and solving the multi-objectives problem for optimal load scheduling of building cluster concerning electricity cost, carbon emission, peak load, and users' satisfaction, particularly when the multiple objectives are conflicting.

To fill the research gaps, this study proposes a MAS-based coordinated optimal load scheduling strategy for building cluster load management in response to dynamic electricity price and marginal emission factor simultaneously. A complex multi-objective optimization problem of conflicts, i.e., minimizing the electricity cost, carbon emissions and peak load while maintaining a good level of users' satisfaction with electricity use, is developed. The multi-objective function is first decomposed into several relatively simplified objective functions and then solved locally in individual component agents. Case study on a campus building cluster is carried out to test and validate the proposed MAS-based load scheduling strategy. One baseline case without DR and three DR schemes are considered in the case study, i.e., price-based DR, MEF-based DR, and hybrid-based DR. The optimization results are systematically and critically compared under two real scenarios with opposite correlations between dynamic electricity price and MEF. The main contributions of this study are summarized as followed.

(1) introduce a more realistic carbon emission factor, i.e., the marginal emission factor, in the building cluster DR management for accurate evaluation of carbon emissions of load scheduling strategies;
(2) develope an optimal load scheduling strategy for building cluster load management considering the MEF and dynamic electricity price simultaneously in DR;
(3) discovere the influences of MEF and dynamic electricity price correlation on the performance of building cluster optimal load scheduling for DR; and
(4) develop a multi-objective function decomposition method and distributed optimization method based on the ADMM algorithm to solve the multi-objective optimization problem of building cluster DR in a distributed manner.

2. Methodology

This study presents a MAS-based coordinated optimal load scheduling strategy. The performance of the proposed strategy is evaluated under different scenarios. The methodology framework of the MAS-based coordinated optimal load scheduling strategy is shown in Fig. 2.

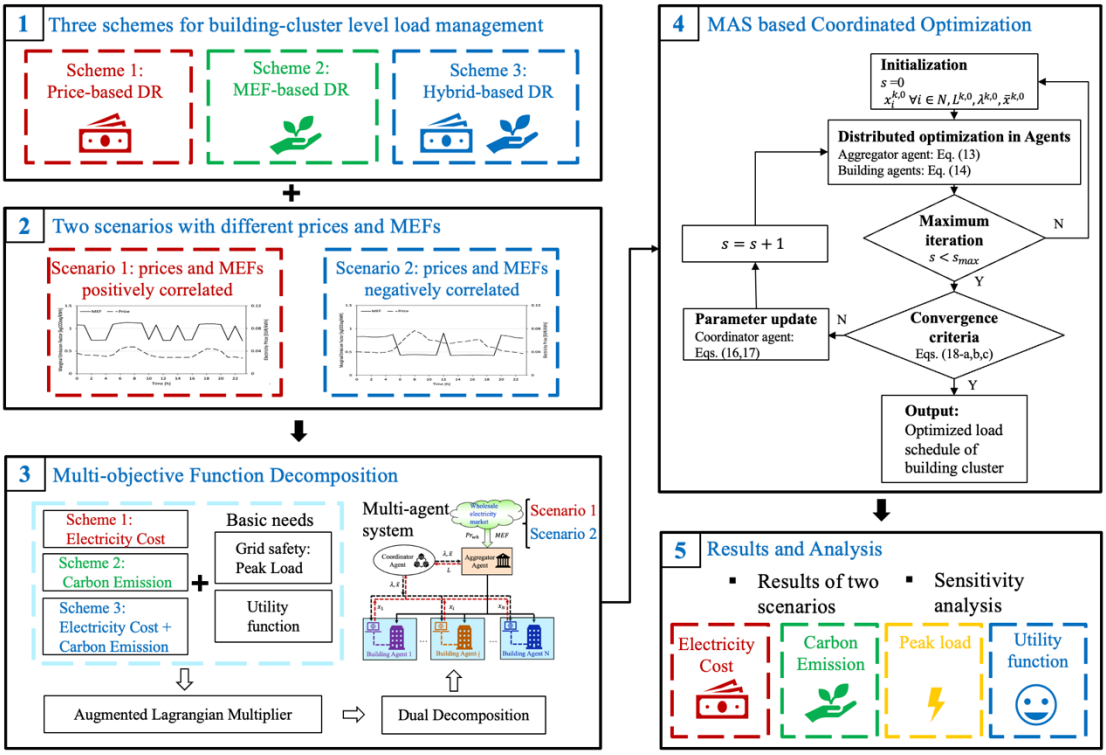

Fig. 2. Methodology framework of the proposed MAS-based coordinated optimal load scheduling strategy

Specifically, scheme 1 is to implement load management from the perspective of electricity cost. The dynamic electricity price will be considered in scheme 1. Price-based DR will be conducted to minimize the electricity cost using dynamic electricity price, but the carbon emission will be ignored in the optimization. Scheme 1 is the one that commonly adopted in the past studies. Scheme 2 is from the perspective of carbon emission. MEF-based DR will be conducted to minimize the carbon emission using MEF, while the electricity cost will be ignored. Scheme 3 is from the perspective of both electricity cost and carbon emission. Both dynamic electricity prices and MEFs will be adopted simultaneously in scheme 3 to minimize both electricity cost and carbon emission, which is proposed for the first time in this paper. This kind of DR is called hybrid-based DR. Since the dynamic electricity prices may positively or negatively

correlated with the MEFs, the performance for the three schemes of DR under the two scenarios, i.e., scenario 1 (positively correlated) and scenario 2 (negatively correlated), will be evaluated. Another two basic objectives in the operation of the building cluster, i.e., peak load and utility function, are also considered to meet the basic needs of grid safety and utility function.

The MAS approach is adopted to realize the optimal coordinated load scheduling for building cluster DR. The complex interactions among multiple parties in a building cluster, including the management company and individual buildings are captured, and the complex multi-objective optimization problem is formulated. The steps for implementing the MAS-based optimal coordinated load scheduling of building cluster is described as follows. Firstly, the multi-objective function is decomposed into several relatively simple objective functions using the methods of Augmented Lagrangian Multiplier and dual decomposition (introduced in section 2.3). Secondly, the simple objective functions are assigned to each agent in the MAS. Thirdly, the coordinated optimizations are conducted locally in each agent. Finally, the local optimization problems are solved using Alternating Direction Method of Multipliers (ADMM) algorithm, and the optimal solutions, i.e., the optimal load schedules of individual buildings and the entire building cluster, are obtained. The details of each step are elaborated in section 2.2-2.4. The performance of the three schemes under the two scenarios will be comprehensively and critically analyzed in terms of electricity cost, carbon emission, peak load, and utility function in section 4.1-4.2. The sensitivity analysis of the parameter of utility function (introduced in section 2.2) and weighting factors of peak load are conducted in section 4.3.

2.1 Description of the MAS

The schematic and principle of the proposed MAS is shown in Fig.3. The MAS consists of two kinds of agents, i.e., component agents and coordinator agent. Component agents include the aggregator agent and building agents. The aggregator agent has two tasks. First, the aggregator agent is responsible for facilitating the electricity transaction between individual buildings and the wholesale electricity market. Second, the

aggregator agent optimizes the day-ahead hourly aggregated load schedules ($\{L^k\}_{k=1}^K$) for the building cluster DR based on the day-ahead hourly electricity prices ($\{Pr_{wh}^k\}_{k=1}^K$) and hourly MEFs ($\{MEF^k\}_{k=1}^K$). After trading completed in the day-head wholesale electricity market, the electricity prices and MEFs will be determined, which will then be obtained by the aggregator agent. Each individual building *i* in a building cluster is considered as a building agent. The task of the building agent is to optimize the day-ahead hourly load schedules of the individual building ($\{x_i^k\}_{k=1}^K, i \in N$). Here, *N* is the total number of individual buildings, and *K* is the total number of time slots in a day and is set to 24.

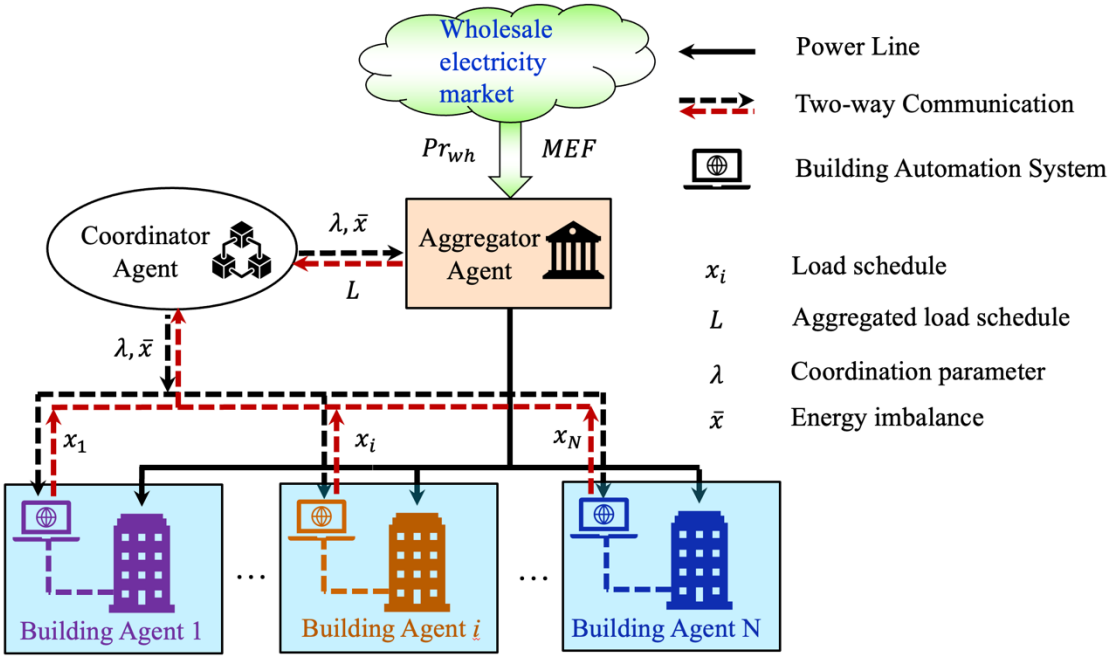

Fig. 3. Schematic of the proposed MAS

The coordinator agent is responsible for updating and broadcasting the coordination parameters to facilitate achieving the coordinated optimal results. If the aggregator agent and building agents are isolated and conduct optimization individually without effective coordination, the energy balance constraint may not be satisfied and the optimization of multiple objectives may not be achieved. The coordinator agent will ensure the satisfaction of the energy balance constraint and achieve multi-objective optimization by conducting energy imbalance ($\bar{x}^k$) calculation, coordinate parameter (λ^k) update and convergence criteria ($\varepsilon_1, \varepsilon_2$) judgement. The coordinate parameter (λ^k) and the convergence criteria ($\varepsilon_1, \varepsilon_2$) are defined in section 2.3 and 2.4 respectively.

2.2 Optimization objectives

Multiple objectives including electricity cost, carbon emission, peak load and utility function on electricity usage are considered in the MAS-based optimal load scheduling strategy for building cluster DR. The multiple objectives are decomposed into several relatively simple sub-objectives and assigned to different component agents to perform distributed optimization.

2.2.1 Optimization objectives

(1) Electricity cost

The electricity cost (C^k) refers to the payment of the building cluster to the day-ahead wholesale electricity market when building cluster buy certain amount of electricity under the wholesale electricity price at time slot k [41]. The total electricity cost is determined by the aggregated hourly electricity load and the corresponding wholesale electricity price [41], as shown in Eq. (1).

$$C^k = Pr_{wh}^k \cdot L^k \tag{1}$$

where Pr_{wh}^k is the day-ahead wholesale electricity price at time slot k. L^k is the aggregated load schedule at time slot k..

(2) Carbon emission

The electricity-related carbon emission (CE^k) refers to the emission imported from the grid. At time slot k, the carbon emission of the building cluster is determined by the aggregated hourly electricity load and the emission factor. This study adopts the MEFs for more accurate calculation of carbon emission when implementing building cluster DR. The carbon emission of building cluster is calculated by Eq. (2) [40].

$$CE^k = MEF^k \cdot \left(L^k - L_0^k\right) \tag{2}$$

where MEF^k is the marginal emission factor of the imported electricity at time slot k. L_0^k is the aggregated baseline power load of building cluster without DR at time slot k.

(3) Peak load

The peak load (PL) refers to the maximum aggregated load of the building cluster over the *K* time slots [47] and is considered in this study to address the basic need of grid safety. The peak load of aggregator agent is shown in Eq. (3).

$$PL = max\ \{L^k\}_{k=1}^{K} \tag{3}$$

It should be noted that the *max* operation should be linearized before carrying out optimization. In this study, the standard linearization procedure (Eqs. (4-5)) as recommended in [50] is adopted. First, the continuous variable *z* (Eq. (4)) is introduced to substitute original PL. Second, *K* number of binary variables $\{u^k\}_{k=1}^{K}$ and a sufficient large variable M (set as 10000) (Eq. (5)) are introduced to constraint the continuous variable *z*. It can be proved mathematically that the Eq. (3) and Eqs. (4-5) are equivalent [50].

$$PL = z \tag{4}$$

$$s.t. \begin{cases} z \le L^k, k = 1 \dots K \\ L^k \le\ z - M \cdot (1 - u^k)\ , k = 1 \dots K \\ \sum_{k=1}^{K} u^k \ge 1 \\ u^k \in \{0,1\}, k = 1 \dots K \end{cases} \tag{5}$$

(4) Utility function

"Utility" is a concept that quantifies the level of users' satisfaction for consuming a certain amount of resources which is commonly adopted in economics [51- 54]. Utility function (U_i) expresses the utility as a function of the amount of the resource consumed [55]. A typical resource concerned in DR applications is the electricity. To this end, this study defines a utility function to measure the level of users' satisfaction with electricity use based on the difference between the baseline electric load and the load after load shifting. Utility functions were used to solve the optimal operation problem of air conditioning systems [56] and optimal real-time pricing problem [57]. This study adopts a commonly used quadratic utility function [42], as shown in Eq. (6). The utility sacrifice (S_i^k) is defined as the difference between the baseline load without DR and the load after DR [42], which reflects the sacrifice of the electricity users (i.e., buildings in this study) in adopting DR strategies, as shown in Eq. (7).

$$U_i^k(x_i^k) = \omega_i \cdot x_{0,i}^k \cdot x_i^k - \frac{\omega_i}{2}(x_i^k)^2 \quad (6)$$

$$S_i^k = U_i^k\left(x_{0,i}^k\right) - U_i^k\left(x_i^k\right) = \frac{\omega_i}{2}(x_{0,i}^k - x_i^k)^2 \quad (7)$$

where $x_{0,i}^k$ is the baseline power load of building i at time slot k, x_i^k is the load of building i at time slot k after load shifting. ω_i is a pre-determined constant parameter, which represents the preference of electricity use of building i to shift the power load, $\omega_i > 0$. If a building user have higher ω_i, it means that the user is more reluctant to change electricity use. The influence of the parameter of utility function ω_i on the performance of building cluster load management will be discussed in Section 4. The goal of each building agent is to minimize its utility sacrifice over the *K* time slots.

In this study, each building agent can change the power demand and shift load in a day in response to the dynamic electricity prices and MEFs. It is assumed that the daily total energy consumption of each building agent is constant before and after load shifting, as shown in Eq. (8-a) [42]. The shifted loads are not allowed to exceed the upper limit of flexible load capacity of each building, as shown in Eq. (8-b) [42]. $B_{up,i}^k$ is the upper limit of flexible load capacity of building i at time slot k.

$$s.t.\begin{cases} \sum_{k=1}^{K} x_i^k = \sum_{k=1}^{K} x_{0,i}^k & \text{(8-a)} \\ \left|x_i^k - x_{0,i}^k\right| \le B_{up,i}^k & \text{(8-b)} \end{cases}$$

2.2.2 Description of multiple conflicting objectives

The optimal load scheduling aims to find an optimal solution that minimizes the electricity cost, the carbon emissions, peak load while maintaining the utility function. In other words, the objectives are to effectively balance the multiple conflicting objectives. The following three set of conflicting objectives are included in this study.

(1) Conflicting objective between electricity cost and carbon emissions: as mentioned in the introduction section, when the MEFs are negatively correlated with dynamic electricity prices, price-based load shifting will lead to increased emissions. Such a conflicting objective issue was seldom considered in previous studies.

(2) Conflicting objective between electricity cost/carbon emissions and peak load: when each building independently carries out load shifting based on the electricity prices or MEFs without effective coordination, it will cause a sharp increase of power load during the valley periods of electricity prices or MEFs, thus significantly rising the aggregated peak load.

(3) Conflicting objective between electricity cost/ carbon emission and utility function on the electricity usage: the pursuit of electricity cost reduction or carbon emission reduction will have negative impact on utility function.

Thus, to balance the multiple conflicting objectives, the overall objective function (J) of the building cluster is adopted considering the weighting factor (α, β, γ, θ) of each objective, as shown in Eq. (9) [47]. The overall objective function will be minimized to obtain the optimal load schedule. The constraints of the optimization problem are expressed in Eq. (10).

$$\min J = \alpha \cdot \sum_{k=1}^{K} C^k + \beta \cdot \sum_{k=1}^{K} CE^k + \gamma \cdot PL + \theta \cdot \sum_{i=1}^{N} \sum_{k=1}^{K} S_i^k \quad (9)$$

$$s.t. \sum_{i=1}^{N} x_i^k = L^k \quad (10)$$

In this study, the ADMM based distributed optimization method is adopted to obtain the optimization solution between multiple conflicting objectives for building cluster DR. ADMM is a computing framework especially suitable for solving distributed convex optimization problems. ADMM decomposes the large global problem into several smaller and easier to solve local sub-problems through the process of decomposition and coordination, and obtains the solution of the large global problem by coordinating the solutions of the sub-problems.

2.3 Distributed optimization method

To obtain a coordinated optimization solution for multiple objective function, the distributed optimization and decision making is firstly conducted for each component agent. The objective function of each component agent can be reformulated by using the decomposition theory, which provides the mathematical method to decompose the original problem into sub-problems [31]. The multiple objective function in Eq. (9)

with the energy balance constraint ($\sum_{i=1}^{N} x_i^k = L^k$) can be converted into an unconstraint problem by using the Lagrangian relaxation, as expressed in Eq. (11).

$$\min\ J(x_i, L;\ \lambda) = \alpha \cdot \sum_{k=1}^{K} C^k + \beta \cdot \sum_{k=1}^{K} CE^k + \gamma \cdot PL + \theta \cdot \sum_{i=1}^{N}\sum_{k=1}^{K} S_i^k + \sum_{k=1}^{K} \lambda^k \left(\sum_{i=1}^{N} x_i^k - L^k \right) + \sum_{k=1}^{K} \frac{\rho}{2} \left(\sum_{i=1}^{N} x_i^k - L^k \right)^2 \tag{11}$$

where $J(x_i, L;\ \lambda)$ is the Augmented Lagrangian of the original objective function. λ^k is the Lagrange's multiplier, which is the coordinate parameters of the proposed MAS. ρ is a penalty factor of Augmented Lagrange's multiplier for enhancing the robustness when solving the distributed optimization problem. The primal problem (Eq. (11)) can be solved by introducing the dual problem (Eq. (12)). Since the Eq. (11) is strictly convex and the strong duality holds, the optimal values of the primal and dual problems are the same. The primal optimal point (x_i^{*k}, L^{*k}) can be recovered from the dual optimal point (λ^{*k}).

$$\max\ H(\lambda) = \inf_{\{x_i^k\}_{k=1}^{K}, \{L^k\}_{k=1}^{K}} \{\alpha \cdot \sum_{k=1}^{K} C^k + \beta \cdot \sum_{k=1}^{K} CE^k + \gamma \cdot PL + \theta \cdot \sum_{i=1}^{N}\sum_{k=1}^{K} S_i^k + \sum_{k=1}^{K} \lambda^k \left(\sum_{i=1}^{N} x_i^k - L^k \right) + \sum_{k=1}^{K} \frac{\rho}{2} \left(\sum_{i=1}^{N} x_i^k - L^k \right)^2 \} \tag{12}$$

The terms in Eq. (12) is substituted with Eqs. (1, 2, 3, 7) and the optimization variables x_i^k and L^k are separated as expressed in Eq. (13). The global optimization problem can then be decomposed into a number of sub-problems. Each sub-problem deals with the optimization of an individual agent with a given λ.

$$\min_{\{x_i^k\}_{k=1}^{K}, \{L^k\}_{k=1}^{K}} \left[\alpha \cdot \sum_{k=1}^{K} Pr_{wh}^k \cdot L^k + \beta \cdot MEF^k \cdot \left(L^k - L_0^k \right) - \lambda^k L^k + \gamma \cdot z \right] + \left[\theta \cdot \sum_{i=1}^{N}\sum_{k=1}^{K} \frac{\omega_i}{2} \left(x_{0,i}^k - x_i^k \right)^2 + \lambda^k x_i^k \right] + \sum_{k=1}^{K} \frac{\rho}{2} \left(\sum_{i=1}^{N} x_i^k - L^k \right)^2 \tag{13}$$

For the aggregator agent, the aggregated electricity dispatch ($\{L^k\}_{k=1}^K$) is updated using the objective function shown in Eq. (14). For each of building agent, the electricity schedule ($\{x_i^k\}_{k=1}^K$) is updated using Eq. (15). Eq.(14) and Eq. (15) are equations to solve the primal problem. It is solved in a distributed way in different component agents.

$$\{L^{k,s+1}\}_{k=1}^K := \underset{\{L^k\}_{k=1}^K}{\operatorname{argmin}} \sum_{k=1}^{K} \alpha \cdot Pr_{wh}^k \cdot L^k + \beta \cdot MEF^k \cdot (L^k - L_0^k) - \lambda^{k,s} L^k + \frac{\rho}{2}\left(L^k - (L^{k,s} - \bar{x}^{k,s})\right)^2 + \gamma \cdot z \tag{14}$$

$$\{x_i^{k,s+1}\}_{k=1}^K := \underset{\{x_i^k\}_{k=1}^K}{\operatorname{argmin}}\, \theta \sum_{k=1}^{K} \frac{\omega_i}{2}(x_{0,i}^k - x_i^k)^2 + \lambda^{k,s} x_i^k + \frac{\rho}{2}(x_i^k - (x_i^{k,s} - \bar{x}^{k,s}))^2 \tag{15}$$

The coordinator agent calculates the average energy imbalance $\bar{x}^k$ and updates the coordinate parameter λ^k by Eq. (16) and Eq. (17) respectively to meet the requirement of energy balance constraint [31,43,50]. The average energy imbalance $\bar{x}^k$ term is introduced to realize the separation of the Augmented Lagrange's multiplier term into different distributed optimization equations [31]. The coordinator agent also updates the coordinate parameter λ^k, which is the Lagrange's multiplier, by solving the dual problem using the dual ascent method [31] as shown in Eq. (17). The superscript *s* in Eq. (14-17) represents the number of the iteration step.

$$\bar{x}^{k,s} = \frac{1}{N+1}\left(\sum_{k=1}^{K} x_i^{k,s} - L^{k,s}\right) \tag{16}$$

$$\lambda^{k,s+1} := \lambda^{k,s} + \rho \bar{x}^{k,s} \tag{17}$$

Through the distributed update of the optimization variables (x_i^k and L^k), coordinate parameter λ^k, and average energy imbalance $\bar{x}^k$ as well as the communication between the different agents, the MAS gradually obtain the optimal value until the convergence criteria is reached

2.4 Convergence criteria

The convergence criteria consist of judging the primal residual and dual residuals [31]. The primal residual is calculated by Eq. (18-a), which reflects the energy balance constraint violation. The dual residuals reflect the difference between the current and last values of each optimized variable and are expressed in Eq. (18-b) for aggregator agent and Eq. (18-c) for building agents.

$$\bar{x}^{k,s} \leq \varepsilon_1 \tag{18-a}$$

$$(L^{k,s} - L^{k,s-1})^2 \leq \varepsilon_2 \tag{18-b}$$

$$(x_i^{k,s} - x_i^{k,s-1})^2 \leq \varepsilon_2 \tag{18-c}$$

where, ε_1 and ε_2 are the pre-set stopping threshold, and $\varepsilon_1 = \varepsilon_2 = 0.0001$ in this study. The flow chart of the optimal load scheduling strategy by adopting the ADMM algorithm is presented in Fig. 4.

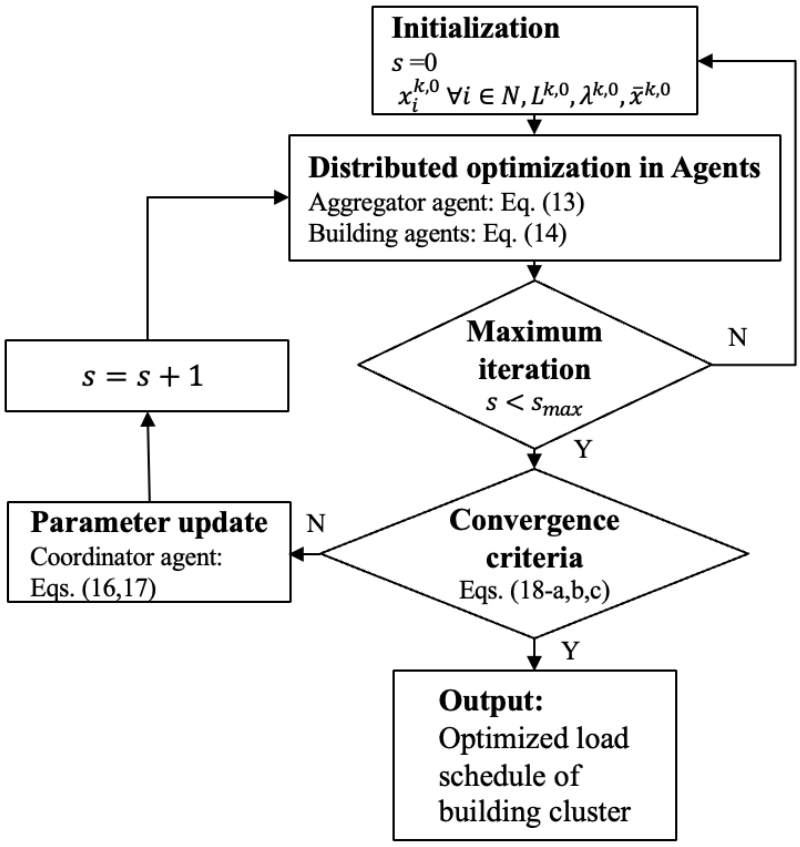

Fig. 4. Flowchart for the solution identification using ADMM

For each step of iteration, each building agent optimizes the load schedule to maximize its utility function. The aggregator agent optimizes the aggregated load schedule to minimize the electricity cost, carbon emission and aggregated peak load. The distributed optimizations in different component agents are conducted in parallel. The optimization solver Gurobi [58] is adopted to solve the distributed optimization problems. The coordinator agent updates the parameters, λ^k and $\bar{x}^k$, to reduce the constraint violation, i.e. to meet the requirement of energy balance constraint. Such an iteration process will be stopped until reaching the pre-set stop threshold (Eqs. 17), or the maximum iteration number is reached. The maximum iteration number is pre-set to be 2000 in this study.

3. Case study

The proposed coordinated optimal load scheduling strategy is tested using the data of a building cluster in a university campus in Hong Kong. Hong Kong is a modern city located in the sub-tropical region with high power demand density and a heavy use of air-conditioning systems. The campus building cluster with a total site area of 94,600 m^2 are equipped with building automation system for monitoring and controlling the facilities operation in buildings. Four building blocks with different functions, such as classrooms, laboratories, offices and library, are selected as the different building agents. The layout and main functions of the selected buildings are presented in Fig. 5. The electricity load profiles of these four buildings on July 3, 2015, as shown in Fig. 6, are adopted to test the proposed strategy for building cluster demand management. In the case study, the four buildings are considered as 4 building agents. The aggregator agent, for example the campus building management office, buys electricity from the day-ahead wholesale electricity market and dispatch to each building. It is assumed that the DR of the building cluster will not influence the electricity prices of whole-sale electricity market and MEFs of electricity grid. It should be noted that although four buildings are selected for testing, the proposed strategy can be also used for optimal load scheduling of building clusters with more buildings. The method proposed in this

paper is generic and it takes the load characteristics data as external parameters, thus it is valid for buildings with different load characteristics.

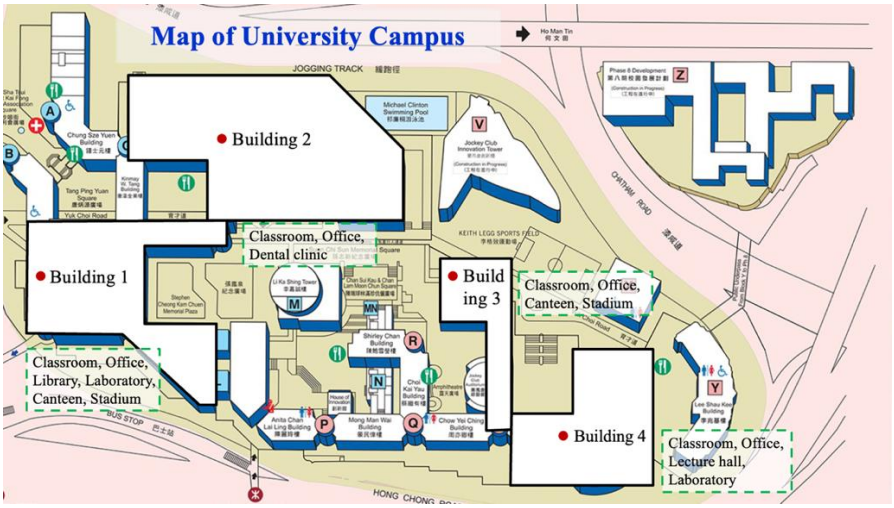

Fig. 5. The layout and functions of the adopted buildings in a university campus

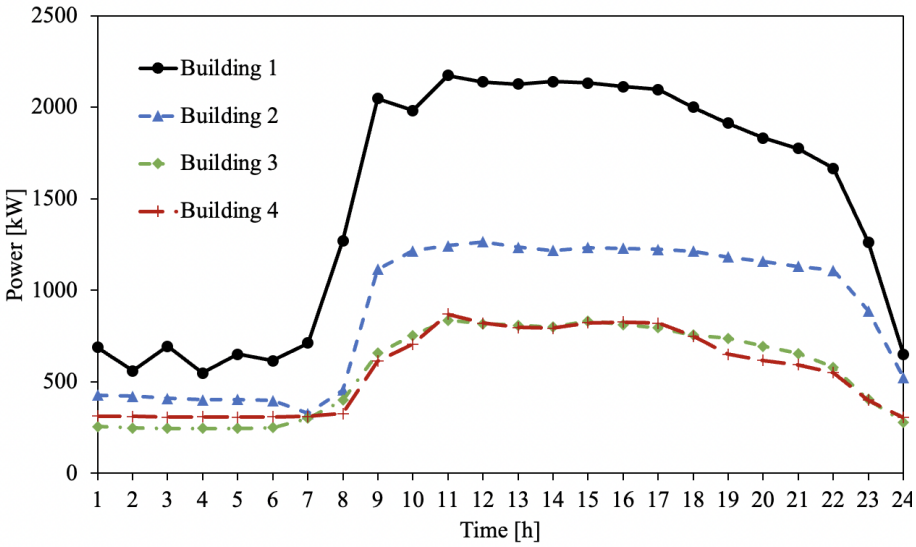

Fig. 6. Historical electricity uses of the four building agents

Since the day-ahead dynamic electricity pricing scheme is not implemented in Hong Kong currently and MEFs data of Hong Kong are also not available, the electricity prices and MEFs data of the Germany's electricity market [20] are adopted. It should be noted that the proposed MAS-based optimal load scheduling strategy takes the electricity prices and MEFs data as external parameters. Therefore, although the data of Germany's electricity market are adopted for testing, the proposed strategy can be applied in other dynamic electricity market. Due to the dynamic electricity prices may

positive or negative correlation with the MEFs [16, 42], two scenarios, i.e. positive scenario and negative scenario are considered in this study. The Pearson correlation coefficient is used to quantify the correlation between electricity prices and MEFs. The day-ahead electricity prices and MEFs data of Mar. 6, 2019, and Dec. 3, 2019, are adopted as the two representative scenarios, as shown in Fig. 7(a) and Fig. 7(b) respectively. The Pearson correlation coefficients between the electricity prices and MEFs are 0.68 and -0.78 for scenario 1 (positive correlation) and scenario 2 (negative correlation), respectively.

(1) In scenario 1 (see Fig. 7 (a)), the valley hours of electricity prices are in the early morning (before 6:00), afternoon (12:00-17:00), and night (after 22:00), and the valley hours of MEFs is basically in consistent with electricity prices, though some fluctuations occur in afternoons. The average of MEFs and electricity prices in scenario 1 is 0.948 kgCO2eq/kWh and 0.035 EUR/kWh, respectively. The standard deviation (STD) of MEFs and electricity prices in scenario 1 is 0.179 kgCO2eq/kWh and 0.0065 EUR/kWh, respectively.

(2) In scenario 2 (Fig. 7 (b)), variation patterns of MEFs and dynamic electricity prices are reversed. The valley hours of electricity prices are still in the early morning (before 7:00) and night (after 20:00), while these time slots are in consistent with the peak hours of MEFs. The average of MEFs and electricity prices in scenario 2 is 0.618 kgCO2eq/kWh and 0.051 EUR/kWh, respectively. The STD of MEFs and electricity prices in scenario 2 is 0.207 kgCO2eq/kWh and 0.0115 EUR/kWh, respectively.

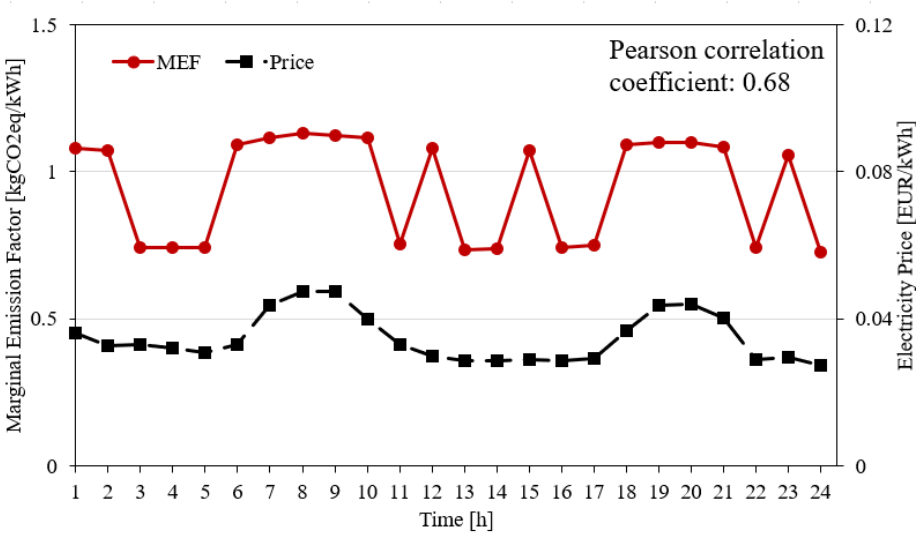

(a) Scenario 1 the electricity prices and MEFs are positively correlated

(b) Scenario 2 the electricity prices and MEFs are negatively correlated

Fig. 7. The day-ahead electricity prices and marginal emission factors of the two scenarios [59]

The parameters of the utility function (ω_i) are set to be 0.001 for each building agent. The weighting factor of peak load objective (γ) is set to be 1. The impact of the ω_i and γ on the optimization results will be discussed in Section 4.3.1 and Section 4.3.2 respectively. The flexible load capacity is assumed to be 0.2 times of baseline load ($B_{up,i}^k = 0.2x_{0,i}^k$). Three schemes are considered for building cluster load management:

(1) Priced-based DR scheme: The aggregator agent will optimize the load schedule to minimize the electricity cost but ignore the carbon emission. The weighting factor α is set as 10 and β is set as 0.

(2) MEF-based DR scheme: The aggregator agent will optimize the load schedule to minimize the carbon emission but ignore the electricity cost. The weighting factor α is set as 0 and β is set as 1.

(3) Hybrid-based DR scheme: The aggregator agent will optimize the load schedule to minimize the carbon emission as well as electricity cost simultaneously. The weighting factor α is set as 5 and β is set as 0.5.

4. Results and discussions

In this section we present the performance of the three DR schemes using MAS-based optimal load scheduling strategy under two scenarios in terms of electricity cost, carbon emission, peak load and utility function. The impacts of some key parameter, such as

the utility function and weighting factors, on the optimization results are analyzed. The limitations of the strategy are discussed at the end of this section.

4.1 Scenario 1: Positively correlated dynamic electricity prices and MEFs

Fig. 8 presents the optimized aggregated power demand schedule of the building cluster under three DR schemes. As shown in the figure, the hourly aggregated power demand is equal to the total power demands of four building agents. For the price-based DR, compared with the baseline of the aggregated power demands, the power load is shifted from peak-price periods (7:00-9:00 and 18:00-20:00) to the valley-price periods (before 6:00 and after 21:00). The peak power demand in the daytime is reduced from 5126 kW to 4821 kW, as the result of peak load reduction. For the MEF-based DR, compared with the baseline, the power demand is partly shifted to the early morning (3:00 to 6:00), afternoon (12:00-17:00), and night (after 22:00) when the MEF is in the valley period (i.e., around 0.75 kgCO2eq/kWh). The daily peak power demand increases from 5126 kW to 5330 kW. This is because the benefits of carbon emission reduction implementing MEF-based DR may offset the disadvantage of peak load increasement. For the hybrid-based DR, the aggregated power demands shifting depends on the variation of MEFs and dynamic electricity prices simultaneously.

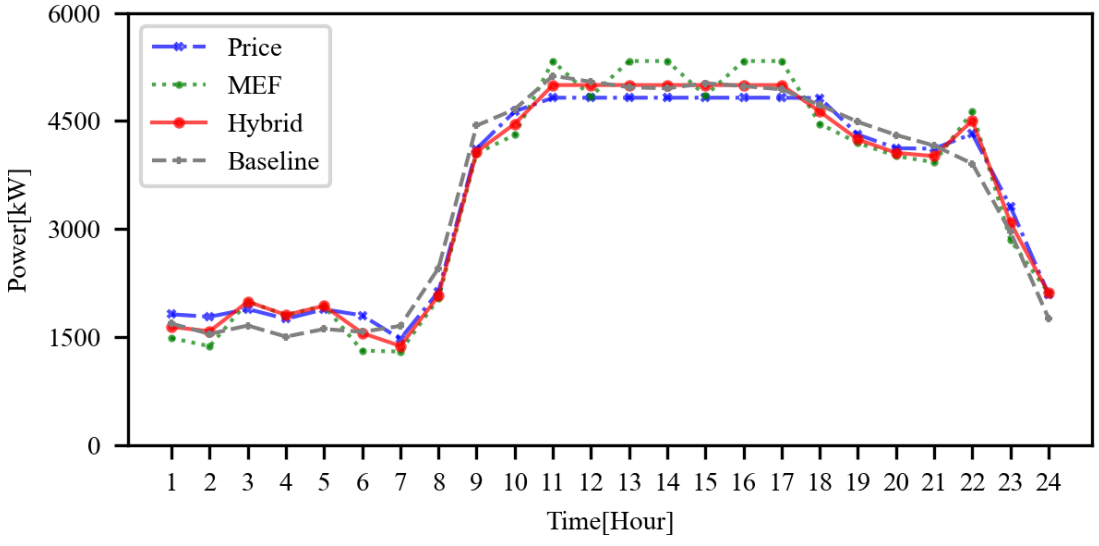

Fig. 8. Optimized aggregated load schedule of building cluster DR under scenario 1

Table 2 Comparison of load scheduling strategy for three DR schemes under scenario 1

DR Scheme	Utility	Utility sacrifice		Electricity cost	Saving	
			%	EUR	EUR	%
Baseline	51740.1	0.0	-	2914.0	-	-
MEF	51390.5	349.5	0.68	2876.1	37.8	1.30
Price	51575.1	165.0	0.32	2897.2	16.7	0.57
Hybrid	51555.5	**184.6**	**0.36**	2885.7	**28.3**	**0.97**
DR Scheme	Carbon emission	Reduction		Peak load	Reduction	
	kgCO2eq	kgCO2eq	%	kW	kW	%
Baseline	79608.8	-	-	5126.0	-	-
MEF	78268.0	1340.8	1.68	5330.3	-204.3	-3.99
Price	79331.6	277.2	0.35	4821.4	304.6	5.94
Hybrid	78880.5	**728.3**	**0.91**	4997.0	**129.0**	**2.52**

Table 2 summarizes the benefits and drawbacks of the proposed MAS-based coordinated multi-objective optimal load scheduling strategy for three different DR schemes under scenario 1. It can be found that implementing the proposed optimal load scheduling strategy can achieve decarbonization and economic benefit under all the DR schemes. The highest carbon emission and electricity cost reduction, about 1.68% and 1.30% compared with baseline respectively, can be achieved by MEF-based DR. The reason is that the variation of MEFs (STD 0.179 kgCO2eq/kWh) is dramatically higher than the variation of electricity prices (STD 0.0065 EUR/kWh) for the positive correlation scenario. Therefore, MEF-based DR will shift more amount of load from peak hours to valley hours of MEFs, resulting in higher carbon emission reduction and electricity cost saving, but also resulting in a higher peak load (about 3.99%). Moreover, the hybrid-based DR achieves a compromise between multi-objectives and can be treated as a compromise solution compared with price-based DR and MEF-based DR.

Fig. 9 shows the optimized power shifting of each building agent under three DR schemes. Four buildings show similar load shifting pattern. In general, all the four buildings shift their loads from the higher to lower periods of prices or MEFs to reduce the electricity costs or carbon emissions, respectively. It should be noticed that the loads of four buildings during the price valley period (12:00-17:00) are still shifted to other

periods. This is because that the aggregated peak load occurs in this period, and the proposed optimal load scheduling strategy can avoid overloading, guarantee grid safety, and achieve a coordinated optimization between multi-objectives.

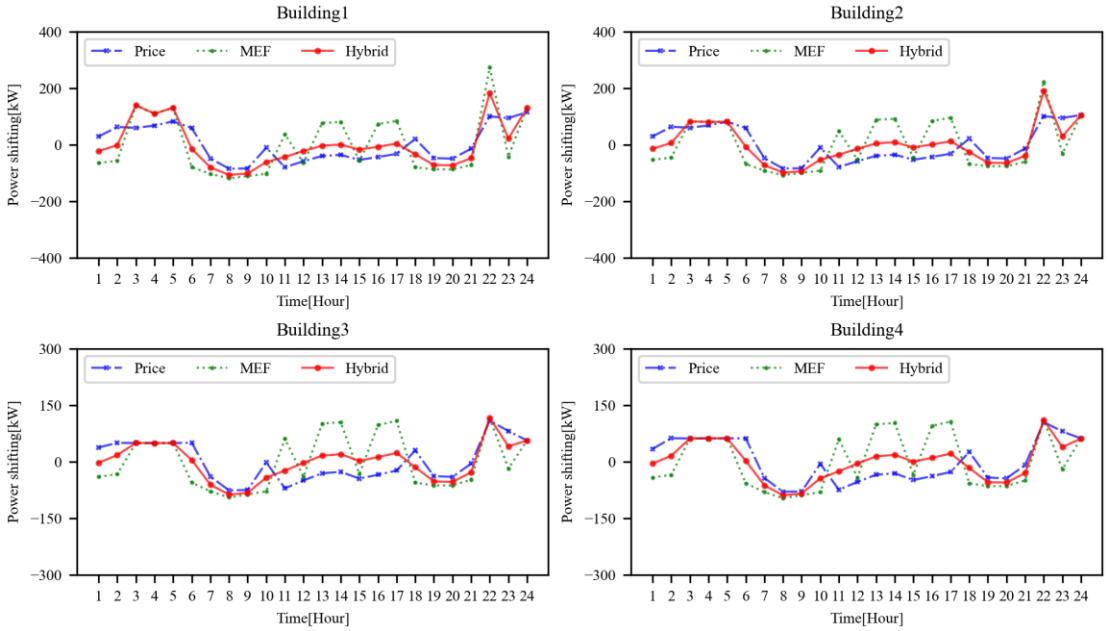

Fig. 9. Optimized power shifting schedule of four building agents under scenario 1

4.2 Scenario 2: Negatively correlated dynamic electricity prices and MEFs

Fig. 10 presents the optimized aggregated power demands schedule of the building cluster DR under scenario 2. The results show that the power shifting pattern of the price-based DR is basically opposite to that of the MEF-based DR due to the negative correlation between dynamic electricity price and MEF. For hybrid-based DR, considering the conflicting objectives of electricity cost and carbon emission, the power load is shifted from afternoon (11:00-17:00) to morning (7:00-9:00) and night (18:00-21:00).

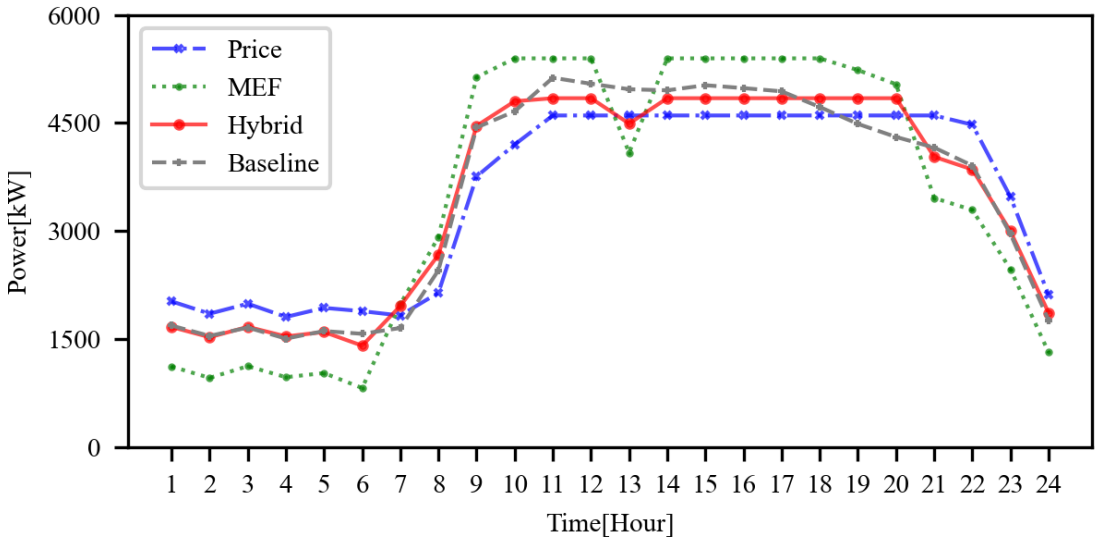

Fig. 10. Optimized aggregated load schedule of building cluster DR under scenario 2

Table 3 summarizes the benefits and drawbacks of optimal load scheduling strategy for three different DR schemes under scenario 2. When the electricity prices and MEFs are negatively correlated, only considering one objective (electricity cost or carbon emission) for load scheduling will results in an opposite variation trend for another objective. For the MEF-based DR, the carbon emission reduces by 5.75% compared with baseline, while the electricity cost increases by 2.63%. For the price-based DR, electricity cost reduces by 2.07%, while the carbon emission increases by 2.78%, compared to the baseline. In this scenario, the electricity cost saving and carbon emission reduction are not significant compared with the baseline case due to the extremely opposite variations in the dynamic electricity prices and MEF. When the price is lower, the MEF is higher. It is a critical challenge to the optimization problem. The MAS-based load scheduling strategy manages to achieve a compromise between the electricity cost saving and carbon emissions reduction, and significant peak load reduction which lowest sacrifice in utility function.

Table 3 Comparison of load scheduling strategy for three DR schemes under scenario 2

DR scheme	Utility	Utility sacrifice		Electricity cost	Saving	
			%	EUR	EUR	%
Baseline	51740.1	0.0	-	4567.4	-	-
MEF	50697.2	1042.9	2.02	4687.7	-120.3	-2.63

Price	51262.4	477.7	0.92	4472.8	94.6	2.07
Hybrid	51604.6	**135.5**	**0.26**	4566.0	**1.5**	**0.03**
DR Scheme	Carbon emission	Reduction		Peak load	Reduction	
	kgCO2	kgCO2	%	kW	kW	%
Baseline	47661.8	-	-	5126.0	-	-
MEF	44922.8	2739.0	5.75	5395.4	-269.4	-5.26
Price	48986.4	-1324.6	-2.78	4602.4	523.6	10.21
Hybrid	47333.9	**327.9**	**0.69**	4842.2	**283.8**	**5.54**

Fig. 11 shows the optimized power shifting of four building agents for the three DR schemes under scenario 2. In general, the power shifting pattern of four buildings under price-based DR is opposite to results of MEF-based DR. In addition, individual buildings will make their own power shifting decision according to their local information. Comparing the power shifting schedule between building 1 and building 2 for the MEF-based DR, it can be found that the power shifting in building 1 is larger than that in building 2 at 8:00. This is because the morning start-up time in building 1 (7:00) is one hour earlier than that in building 2 (8:00), and both of the 7:00 and 8:00 is the valley period for MEF. Therefore, the building 1 can make full use of the higher load flexibility at 8:00 to shift higher amount of power to exploit the benefit of lower MEF.

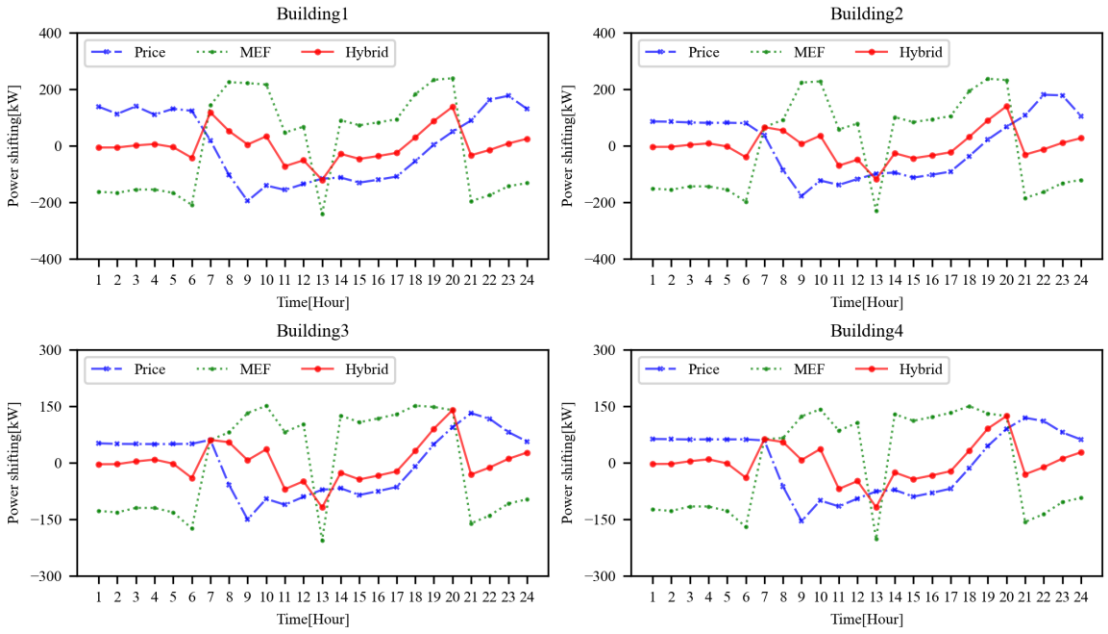

Fig. 11. Optimized load schedule of four building agents under scenario 2.

4.3 Impact of key parameters on load scheduling

The parameter of the user's utility function and weighting factor of peak load objective are the two important factors influencing the results of building cluster load schedule. The impacts of these two parameters are evaluated in this section.

4.3.1 Impacts of parameter of user's utility function

The utility refers to the level of satisfaction of building agents on electricity use. A higher ω_i will lead to more reluctant of the users to change their electricity demand. To investigate the impact of ω_i on the optimization results, this parameter of Building 1 agent is set to be 0.0003, 0.001, 0.003, 0.01 respectively (nearly triple times for each step), while the parameters of other building agents remain unchanged, i.e. $\omega_i = 0.001, i = 2,3,4$. Other global parameters also remain unchanged. Fig. 12 shows the optimized power demands schedule of Building 1 and 2 agents under scenario 2 with the varying parameters of Building 1 agent's utility function. The optimized power demands schedule of Building 3 and 4 agents show similar variation pattern with Building 2; thus, they are not shown. As shown in the figures, this parameter of Building 1 agent also influences the load schedule of Building 2 agent. For Building 1, a higher ω_1 leads to less load shifting, which makes the load curve of Building 1 gradually approach the baseline. The amount of load shifting of Building 2 becomes higher with the increase of ω_1, even though ω_2 remain unchanged.

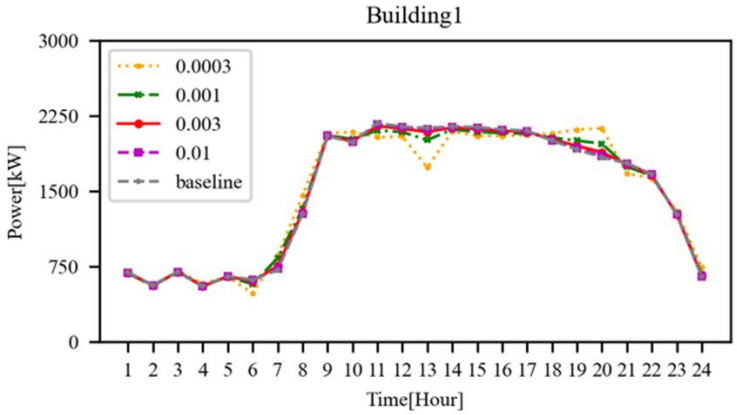

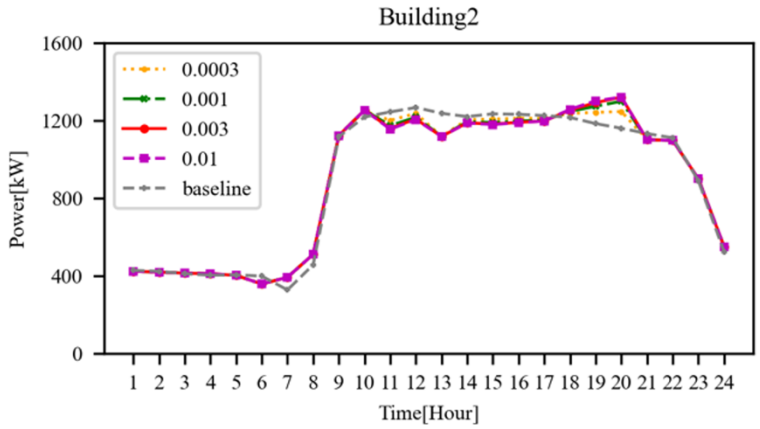

Fig. 12. Optimized power load schedules of Building 1 and 2 agents under scenario 2 with the varying parameters of Building 1.

The impact of ω_i on utility sacrifice, electricity cost, carbon emission and peak load of the building cluster DR are shown in the Table 4. It should be noted that the baseline utilities are different for each case, thus the value of utility in the Baseline row is not presented, and the utility sacrifices of each case are calculated with the corresponding baseline utilities. It can be seen from Table 4 that increasing the ω_i will lead to the decrease of the utility sacrifice, carbon emission, and electricity cost. However, the changes gradually decrease with the geometric increase of ω_i, which means that when the ω_i are small (the users are basically not concern about the load variation), the buildings will show a better energy flexibility.

Table 4 Impacts of parameter of utility function on the performance of building cluster DR

ω_i	Utility	Utility sacrifice		Electricity cost	Saving	
			%	EUR	EUR	%
Baseline	-	-	0.0	4567.4	-	-
0.0003	29418.1	127.2	0.43	4569.3	-1.9	-0.04
0.001	51604.6	135.5	0.26	4566.0	1.5	0.03
0.003	115024.9	128.8	0.11	4565.0	2.4	0.05
0.01	336976.8	124.7	0.04	4564.9	2.5	0.05
ω_i	Carbon emission	Reduction		Peak load	Reduction	
	kgCO2	kgCO2	%	kW	kW	%
Baseline	47661.8	-	-	5126.0	-	-

0.0003	47168.9	492.9	1.03	4854.8	271.2	5.29
0.001	47333.9	327.9	0.69	4842.2	283.8	5.54
0.003	47403.2	258.6	0.54	4847.6	278.4	5.43
0.01	47424.5	237.3	0.50	4852.5	273.5	5.33

4.3.2 Impacts of weighting factor of peak load objective

The weighting factor of peak load objective determines the relative importance of the peak load objective among other objectives. The higher the γ, the more important the peak load. To investigate the impact of γ on the optimization results, the γ is set to be 0.1, 1, 10 respectively. It should be noted that different from the parameters of user's utility function which effect on single building (though also influence other buildings), weighting factor of peak load γ will directly influence the aggregated peak load of building cluster. Fig. 13 presents the optimized total power demands of the building cluster aggregator agent with the varying weighting factor of peak load objective. The peak load significantly drops from 5126 kW to 4429.8 kW when the γ increases from 0.1 to 10.

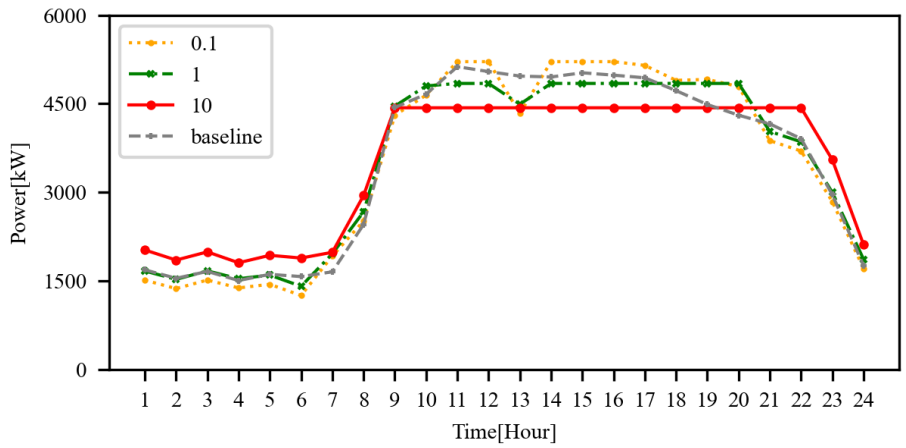

Fig. 13. Optimized aggregated load schedules of the aggregator agent with the varying weighting factors of peak load objective.

Fig. 14 shows the optimized power load schedule of four building agents with the varying weighting factor of peak load objective. Although the peak load of the building cluster drops with the increase of γ, it is not the case for the peak load of each individual building. For example, when the γ is equal to 10, the peak load of Building 2 is actually

higher than the peak load when the γ is equal to 0.1. This means that each building agent can be effectively controlled under the guidance of the coordinator agent to achieve the common goal of aggregated peak load reduction.

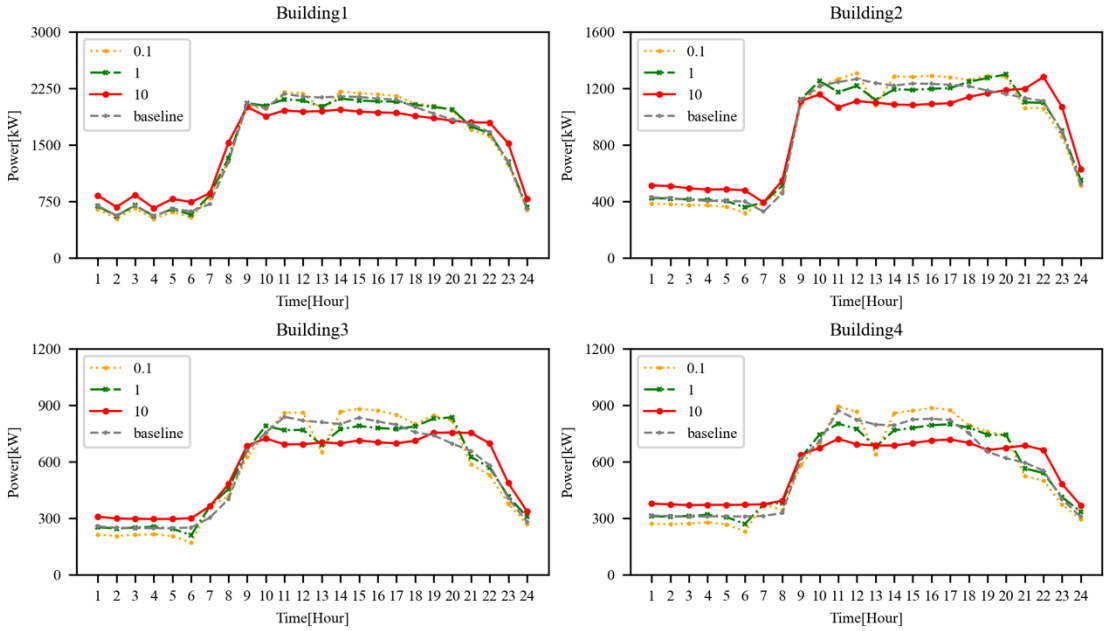

Fig. 14. Optimized load schedules of four building agents with the varying weighting factors of peak load objective.

4.4 Discussions

The price-based DR scheme is commonly adopted to achieve economical operation. Based on the results of the two scenarios, it can be seen that the price-based DR can sometimes result in the increase of carbon emissions, which is inconsistent with the goal of low-carbon operation of the future energy system. Conversely, the MEF-based DR scheme address the decarbonization issue to achieve the maximized carbon reduction, while this scheme may infringe the economic benefits of the aggregator agent. The hybrid-based DR scheme considers both the dynamic electricity prices and the MEFs to achieve decarbonization and cost saving. When the dynamic electricity prices and the MEFs are positively correlated (scenario 1), the effects of hybrid-based DR scheme are similar to the price-based and the MEF-based DR schemes. All the three schemes can achieve the reduction of carbon emissions and electricity cost. Whereas, when the dynamic electricity prices and the MEFs are negatively correlated (scenario 2), the hybrid-based DR scheme can reach a compromise between the price-based and

MEF-based DR schemes, which can still achieve the reduction of carbon emissions and electricity cost, though reductions are relatively low. For the future load management of building cluster towards both decarbonization and economic objectives, the hybrid-based DR scheme will be a better one compared with the price-based DR scheme or the MEF-based DR scheme. It is worth mentioning that the two scenarios extracted from German Electricity Market represent two relatively extreme correlations between dynamic electricity prices and MEF.

Implementing the proposed MAS-based coordinated optimal energy scheduling strategy for building cluster demand response requires good network communication infrastructure. In the multi-agent system, a stable and reliable two-way communication among the aggregator agent, the coordinator agent, and each building agents to exchange data concerning load scheduling, energy imbalance and coordination parameters is essential to successfully implement the proposed strategy. The two-way communication is readily available with the development of communication infrastructure for smart grids and smart cities. The influence of network condition on the convergence of the proposed method in an unstable network environment, as well as methods to accelerate convergence is important to the applicability of the proposed strategy, but not addressed in this study.

The load prediction is critically important to the load scheduling strategies, which is also a very challenging topic. Data-driven models are becoming popular in recent years as they do not need detailed information about buildings and their energy systems, which improve the generalization capability of the models and the model-based strategies in different buildings. As this study focuses on formulating and solving the multi-objective optimization problem considering both dynamic electricity prices and marginal carbon emission factors, it is assumed that the day-ahead predicted load profiles are given as the input of the method. The influences of load prediction uncertainty on the strategy are not considered, which is a limitation to be addressed.

5. Conclusion

This paper presents a hybrid-based DR scheme for building cluster load management and develops a MAS-based coordinated optimal load scheduling strategy to implement

different DR schemes. The MEF is adopted for evaluating the realistic effect of building cluster DR on carbon emissions. The performance of the strategy in a campus building cluster load management under three DR schemes (i.e., price-based DR, MEF-based DR, and hybrid-based DR) are compared in the case study. In addition, the impacts of correlations between MEFs and dynamic electricity prices are analyzed in two scenarios. Real German electricity market data are used to test the proposed coordinated optimal load scheduling strategy. The results show that the price-based DR may result in the rise of carbon emission, and the MEF-based DR can lead to higher electricity cost. The hybrid-based DR can achieve a balance between the goals of electricity cost and carbon emission in both two scenarios, and reduce peak load and maintain utility function at the same time. More detailed conclusions on the performance of the strategies can be drawn as follows.

(1) According to the results of case study, in scenario 1 (electricity price and MEF are positively correlated), all the three DR schemes for load management can reduce electricity cost and carbon emissions simultaneously.

(2) In scenario 2 (negatively correlated), both the price-based DR and MEF-based DR cannot achieve the goals of decarbonization and economy at the same time. The price-based DR can achieve the maximized electricity cost reduction (by 2.07%), while it will result in the increase of carbon emission (by 2.78%). The MEF-based DR can achieve the maximized carbon emission reduction (by 5.75%), but it will lead to the increase of electricity cost (by 2.63%).

(3) In scenario 2 (negatively correlated), both the carbon emission and electricity cost can be reduced (by 0.69% and 0.03% respectively) by implementing the optimal strategy, while reductions are insignificant due to the extreme opposite trends of the price and MEF. Under such a disadvantaged situation, the MAS-based optimal strategy can still reach a compromise of decarbonization and economic benefits.

As discussed, reliable network communication and load predictions are essential to the implementation of the proposed MAS-based optimal scheduling method for building cluster demand response. In future work, uncertainties associated with network communication and load predictions should be considered and addressed in the strategy to improve its robustness against those uncertainties.

Acknowledgements:

The authors gratefully acknowledge the support of this research by the National Key Research and Development Program of China (2021YFE0107400) and Innovation Fund Denmark in relation to SEM4Cities (IFD 0143–0004). The authors also acknowledge IEA EBC Annex 82 for the many fruitful discussions and knowledge exchange.

References

[1] R. Li, A.J. Satchwell, D. Finn, T.H. Christensen, M. Kummert, J. Le Dréau, R.A. Lopes, H. Madsen, J. Salom, G. Henze, K. Wittchen, Ten questions concerning energy flexibility in buildings, Build. Environ. 223 (2022) 109461. https://doi.org/10.1016/j.buildenv.2022.109461.

[2] S.A. Mansouri, A. Ahmarinejad, M.S. Javadi, A.E. Nezhad, M. Shafie-Khah, J.P.S. Catalão, Demand response role for enhancing the flexibility of local energy systems, in: Distrib. Energy Resour. Local Integr. Energy Syst., Elsevier, 2021: pp. 279–313. https://doi.org/10.1016/B978-0-12-823899-8.00011-X.

[3] R. Tang, S. Wang, H. Li, Game theory based interactive demand side management responding to dynamic pricing in price-based demand response of smart grids, Appl. Energy. 250 (2019) 118–130. https://doi.org/10.1016/j.apenergy.2019.04.177.

[4] S.A. Mansouri, A. Ahmarinejad, F. Sheidaei, M.S. Javadi, A. Rezaee Jordehi, A. Esmaeel Nezhad, J.P.S. Catalão, A multi-stage joint planning and operation model for energy hubs considering integrated demand response programs, Int. J. Electr. Power Energy Syst. 140 (2022) 108103. https://doi.org/10.1016/j.ijepes.2022.108103.

[5] R. Tang, H. Li, S. Wang, A game theory-based decentralized control strategy for power demand management of building cluster using thermal mass and energy storage, Appl. Energy. 242 (2019) 809–820. https://doi.org/10.1016/j.apenergy.2019.03.152.

[6] K. Shan, S. Wang, C. Yan, F. Xiao, Building demand response and control methods for smart grids: A review, Sci. Technol. Built Environ. 22 (2016) 692–704. https://doi.org/10.1080/23744731.2016.1192878.

[7] J. Salpakari, J. Mikkola, P.D. Lund, Improved flexibility with large-scale variable renewable power in cities through optimal demand side management and power-to-heat conversion, Energy Convers. Manag. 126 (2016) 649–661. https://doi.org/10.1016/j.enconman.2016.08.041.

[8] Electrical and Mechanical Services Department of Hong Kong, Hong Kong energy end-use data, 2020. https://www.emsd.gov.hk/filemanager/en/content_762/HKEEUD2020.pdf.

[9] A. Satchwell, M. Piette, A. Khandekar, J. Granderson, N. Frick, R. Hledik, A. Faruqui, L. Lam, S. Ross, J. Cohen, K. Wang, D. Urigwe, D. Delurey, M. Neukomm, D. Nemtzow, A National Roadmap for Grid-Interactive Efficient Buildings, 2021. https://doi.org/10.2172/1784302.

[10] K. Shan, J. Wang, M. Hu, D. Gao, A model-based control strategy to recover cooling energy from thermal mass in commercial buildings, Energy. 172 (2019) 958–967. https://doi.org/10.1016/j.energy.2019.02.045.

[11] B. Cui, S. Wang, C. Yan, X. Xue, Evaluation of a fast power demand response strategy using active and passive building cold storages for smart grid applications, Energy Convers. Manag. 102 (2015) 227–238. https://doi.org/10.1016/j.enconman.2014.12.025.

[12] S.A. Mansouri, E. Nematbakhsh, A.R. Jordehi, M. Tostado-Veliz, F. Jurado, Z. Leonowicz, A Risk-Based Bi-Level Bidding System to Manage Day-Ahead Electricity Market and Scheduling of Interconnected Microgrids in the presence of Smart Homes, in: 2022 IEEE Int. Conf. Environ. Electr. Eng. 2022 IEEE Ind. Commer. Power Syst. Eur. EEEIC ICPS Eur., IEEE, Prague, Czech Republic, 2022: pp. 1–6. https://doi.org/10.1109/EEEIC/ICPSEurope54979.2022.9854685.

[13] S.A. Mansouri, A. Ahmarinejad, E. Nematbakhsh, M.S. Javadi, A. Esmaeel Nezhad, J.P.S. Catalão, A sustainable framework for multi-microgrids energy management in automated distribution network by considering smart homes and high penetration of renewable energy resources, Energy. 245 (2022) 123228. https://doi.org/10.1016/j.energy.2022.123228.

[14] T.Q. Péan, J. Salom, R. Costa-Castelló, Review of control strategies for improving the energy flexibility provided by heat pump systems in buildings, J. Process Control. 74 (2019) 35–49. https://doi.org/10.1016/j.jprocont.2018.03.006.

[15] V. Bianco, F. Scarpa, L.A. Tagliafico, Estimation of primary energy savings by using heat pumps for heating purposes in the residential sector, Appl. Therm. Eng. 114 (2017) 938–947. https://doi.org/10.1016/j.applthermaleng.2016.12.058.

[16] C. Roux, P. Schalbart, B. Peuportier, Accounting for temporal variation of electricity production and consumption in the LCA of an energy-efficient house, J. Clean. Prod. 113 (2016) 532–540. https://doi.org/10.1016/j.jclepro.2015.11.052.

[17] J. Clauß, S. Stinner, C. Solli, K.B. Lindberg, H. Madsen, L. Georges, A generic methodology to evaluate hourly average CO2eq. intensities of the electricity mix to deploy the energy flexibility potential of Norwegian buildings, (2018) 20.

[18] M. Capone, E. Guelpa, V. Verda, Multi-objective optimization of district energy systems with demand response, Energy. 227 (2021) 120472. https://doi.org/10.1016/j.energy.2021.120472.

[19] I. Khan, M.W. Jack, J. Stephenson, Analysis of greenhouse gas emissions in electricity systems using time-varying carbon intensity, J. Clean. Prod. 184 (2018) 1091–1101. https://doi.org/10.1016/j.jclepro.2018.02.309.

[20] M. Fleschutz, M. Bohlayer, M. Braun, G. Henze, M.D. Murphy, The effect of price-based demand response on carbon emissions in European electricity markets: The importance of adequate carbon prices, Appl. Energy. 295 (2021) 117040. https://doi.org/10.1016/j.apenergy.2021.117040.

[21] G. Lowry, Day-ahead forecasting of grid carbon intensity in support of heating, ventilation and air-conditioning plant demand response decision-making to reduce carbon emissions, Build. Serv. Eng. Res. Technol. 39 (2018) 749–760. https://doi.org/10.1177/0143624418774738.

[22] P.J.C. Vogler-Finck, R. Wisniewski, P. Popovski, Reducing the carbon footprint of house heating through model predictive control – A simulation study in Danish conditions, Sustain. Cities Soc. 42 (2018) 558–573. https://doi.org/10.1016/j.scs.2018.07.027.

[23] K. Siler-Evans, I.L. Azevedo, M.G. Morgan, Marginal Emissions Factors for the U.S. Electricity System, Environ. Sci. Technol. 46 (2012) 4742–4748. https://doi.org/10.1021/es300145v.

[24] A.D. Hawkes, Estimating marginal CO2 emissions rates for national electricity systems, Energy Policy. 38 (2010) 5977–5987. https://doi.org/10.1016/j.enpol.2010.05.053.

[25] A. Wang, R. Li, S. You, Development of a data driven approach to explore the energy flexibility potential of building clusters, Appl. Energy. 232 (2018) 89–100. https://doi.org/10.1016/j.apenergy.2018.09.187.

[26] I. Vigna, R. Pernetti, W. Pasut, R. Lollini, New domain for promoting energy efficiency: Energy Flexible Building Cluster, Sustain. Cities Soc. 38 (2018) 526–533. https://doi.org/10.1016/j.scs.2018.01.038.

[27] Y. Shoham, K. Leyton-Brown, Multiagent systems: algorithmic, game-theoretic, and logical foundations., Cambridge University Press, 2008.

[28] A. Dorri, S.S. Kanhere, R. Jurdak, Multi-Agent Systems: A Survey, IEEE Access. 6 (2018) 28573–28593. https://doi.org/10.1109/ACCESS.2018.2831228.

[29] M. WOOLDRIDGE, N. Jennings, Intelligent agents: theory and practice, Knowl. Eng. Rev. 10 (1995) 115–152.

[30] H. Rezaee, F. Abdollahi, Average Consensus Over High-Order Multiagent Systems, IEEE Trans. Autom. Control. 60 (2015) 3047–3052. https://doi.org/10.1109/TAC.2015.2408576.

[31] S. Boyd, Distributed Optimization and Statistical Learning via the Alternating Direction Method of Multipliers, Found. Trends® Mach. Learn. 3 (2010) 1–122. https://doi.org/10.1561/2200000016.

[32] M.R. Basir Khan, R. Jidin, J. Pasupuleti, Multi-agent based distributed control architecture for microgrid energy management and optimization, Energy Convers. Manag. 112 (2016) 288–307. https://doi.org/10.1016/j.enconman.2016.01.011.

[33] A. El Zerk, M. Ouassaid, Y. Zidani, Decentralised strategy for energy management of collaborative microgrids using multi-agent system, IET Smart Grid. (2022) stg2.12077. https://doi.org/10.1049/stg2.12077.

[34] S. Boudoudouh, M. Maâroufi, Multi agent system solution to microgrid implementation, Sustain. Cities Soc. 39 (2018) 252–261. https://doi.org/10.1016/j.scs.2018.02.020.

[35] S.A. Mansouri, E. Nematbakhsh, A. Ahmarinejad, A.R. Jordehi, M.S. Javadi, M. Marzband, A hierarchical scheduling framework for resilience enhancement of decentralized renewable-based microgrids considering proactive actions and mobile units, Renew. Sustain. Energy Rev. 168 (2022) 112854. https://doi.org/10.1016/j.rser.2022.112854.

[36] R. Roche, S. Suryanarayanan, T.M. Hansen, S. Kiliccote, A. Miraoui, A multi-agent model and strategy for residential demand response coordination, in: 2015 IEEE Eindh. PowerTech, IEEE, Eindhoven, Netherlands, 2015: pp. 1–6. https://doi.org/10.1109/PTC.2015.7232268.

[37] A. Anvari-Moghaddam, A. Rahimi-Kian, M.S. Mirian, J.M. Guerrero, A multi-agent based energy management solution for integrated buildings and microgrid system, Appl. Energy. 203 (2017) 41–56. https://doi.org/10.1016/j.apenergy.2017.06.007.

[38] J. Cai, D. Kim, R. Jaramillo, J.E. Braun, J. Hu, A general multi-agent control approach for building energy system optimization, Energy Build. 127 (2016) 337–351. https://doi.org/10.1016/j.enbuild.2016.05.040.

[39] L. Zheng, B. Zhou, Y. Cao, S. Wing Or, Y. Li, K. Wing Chan, Hierarchical distributed multi-energy demand response for coordinated operation of building clusters, Appl. Energy. 308 (2022) 118362. https://doi.org/10.1016/j.apenergy.2021.118362.

[40] T. Péan, R. Costa-Castelló, J. Salom, Price and carbon-based energy flexibility of residential heating and cooling loads using model predictive control, Sustain. Cities Soc. 50 (2019) 101579. https://doi.org/10.1016/j.scs.2019.101579.

[41] M. Hu, F. Xiao, J.B. Jørgensen, R. Li, Price-responsive model predictive control of floor heating systems for demand response using building thermal mass, Appl. Therm. Eng. 153 (2019) 316–329. https://doi.org/10.1016/j.applthermaleng.2019.02.107.

[42] P. Samadi, A.-H. Mohsenian-Rad, R. Schober, V.W.S. Wong, J. Jatskevich, Optimal Real-Time Pricing Algorithm Based on Utility Maximization for Smart Grid, in: 2010 First IEEE Int. Conf. Smart Grid Commun., IEEE, Gaithersburg, MD, USA, 2010: pp. 415–420. https://doi.org/10.1109/SMARTGRID.2010.5622077.

[43] N. Li, L. Chen, S.H. Low, Optimal demand response based on utility maximization in power networks, in: 2011 IEEE Power Energy Soc. Gen. Meet., IEEE, San Diego, CA, 2011: pp. 1–8. https://doi.org/10.1109/PES.2011.6039082.

[44] X. Li, J. Wen, A. Malkawi, An operation optimization and decision framework for a building cluster with distributed energy systems, Appl. Energy. 178 (2016) 98–109. https://doi.org/10.1016/j.apenergy.2016.06.030.

[45] M. Hu, F. Xiao, J.B. Jørgensen, S. Wang, Frequency control of air conditioners in response to real-time dynamic electricity prices in smart grids, Appl. Energy. 242 (2019) 92–106. https://doi.org/10.1016/j.apenergy.2019.03.127.

[46] S. Touzani, A.K. Prakash, Z. Wang, S. Agarwal, M. Pritoni, M. Kiran, R. Brown, J. Granderson, Controlling distributed energy resources via deep reinforcement learning for load flexibility and energy efficiency, Appl. Energy. 304 (2021) 117733. https://doi.org/10.1016/j.apenergy.2021.117733.

[47] M. Hu, F. Xiao, Price-responsive model-based optimal demand response control of inverter air conditioners using genetic algorithm, Appl. Energy. 219 (2018) 151–164. https://doi.org/10.1016/j.apenergy.2018.03.036.

[48] J. Niu, Z. Tian, J. Zhu, L. Yue, Implementation of a price-driven demand response in a distributed energy system with multi-energy flexibility measures, Energy Convers. Manag. 208 (2020) 112575. https://doi.org/10.1016/j.enconman.2020.112575.

[49] H. Tang, S. Wang, A model-based predictive dispatch strategy for unlocking and optimizing the building energy flexibilities of multiple resources in electricity markets of multiple services, Appl. Energy. 305 (2022) 117889. https://doi.org/10.1016/j.apenergy.2021.117889.

[50] S.P. Boyd, L. Vandenberghe, Convex optimization, Cambridge University Press, Cambridge, UK ; New York, 2004.

[51] C. Zhang, S. Lasaulce, L. Wang, L. Saludjian, H.V. Poor, A refined consumer behavior model for energy systems: Application to the pricing and energy-efficiency problems, Appl. Energy. 308 (2022) 118239. https://doi.org/10.1016/j.apenergy.2021.118239.

[52] M.-C. A., D.W. M., R.G. J., Microeconomic Theory, 1st ed, Oxford University Press, 1995.

[53] F. LiMam_Belarbi, F.Z. Tahraoui, Optimal Consumption and Investment for Exponential Utility Function, Math. Sci. Appl. E-Notes. 5 (2017) 19–26. https://doi.org/10.36753/mathenot.421478.

[54] R.Y. Chenavaz, I. Pignatel, Utility foundation of a Cobb-Douglas demand function with two attributes, Appl. Econ. 54 (2022) 3206–3211. https://doi.org/10.1080/00036846.2021.2005238.

[55] H. Varian, Microeconomic analysis, 1992.

[56] S. Wang, R. Tang, Supply-based feedback control strategy of air-conditioning systems for direct load control of buildings responding to urgent requests of smart grids, Appl. Energy. 201 (2017) 419–432. https://doi.org/10.1016/j.apenergy.2016.10.067.
[57] Y. Li, J. Li, J. He, S. Zhang, The real-time pricing optimization model of smart grid based on the utility function of the logistic function, Energy. 224 (2021) 120172. https://doi.org/10.1016/j.energy.2021.120172.
[58] https://www.gurobi.com/products/gurobi-optimizer/, (n.d.).
[59] https://github.com/DrafProject/marginal-emission-factors, (n.d.).